Getting the Best out of PRESTO - Part 4: Dispersion Search Discrimination

Peter East

Abstract

The dispersion measure (DM) search plot produced by PRESTO is probably its most important pulsar validation indicator since it can clearly confirm the correct value for the extra-terrestrial source [1,2]. For low signal-to-noise ratio observations the discrimination may not be sufficiently convincing. It has been shown however, that using signal-to-noise ratio (SNR) measure, rather than Chi-square statistic for amplitude sensing, usefully improves DM search discrimination [3]. This article explores a simple technique for further improving DM discrimination and validation confidence by isolating the target pulsar contribution from other random background folded noise peaks.

Introduction

Examining the dispersion characteristic of pulsar candidates in amateur data is an important part of the validation process. With strong signals the professional PRESTO software DM search measure is clear but with weaker signals this is not always so. In fact, below an integrated SNR of about 12:1, the PRESTO *prepfold* output DM plot is often inconclusive. To be fair, PRESTO was designed by professional radio astronomers to detect new pulsars and so is not optimum for validating amateur's weaker detections.

This article follows previous papers recommending peak SNR searching [3,4,5]. It shows that a stronger DM indicator is obtained by comparing the peak SNR search process with a similar search with the pulsar candidate blanked, so isolating the pulsar candidate DM contribution. The solution can be shown to reject folded noise peaks and interference spikes.

Section 1 describes the background principles and examines the ruggedness of the approach by adapting weaker sections of the recorded data to both improve and degrade the candidate final folded SNR.

Section 2 offers some results based on PRESTO-type plots and sub-plots of the three cases for comparison of the usual PRESTO validation features. No method is infallible and for the final result a noise-only example has been handpicked that shows up the limitations of basic pulsar validation schemes.

Section 3 summarizes the developments described.

***Section 1*. Dispersion Search Discrimination**

Pulsar Dispersion

Broadband pulsar signals propagating the interstellar medium interact with free electrons to lower its group velocity, effectively delaying the lower frequency components. For a given pulsar radio frequency and RF band, it is convenient to describe the band dispersion as the dispersion in ms/MHz bandwidth as a function of the RF centre frequency f_0 (in MHz). For the RF band and receiver bandwidth chosen, dispersion time t_d is calculated from,

$$t_d = 8.3.DM.\left(\frac{1}{f_0^3}\right).10^6 \quad ms/MHz \qquad (1)$$

DM is the catalogued pulsar dispersion measure (= 26.7 for B0329+54).

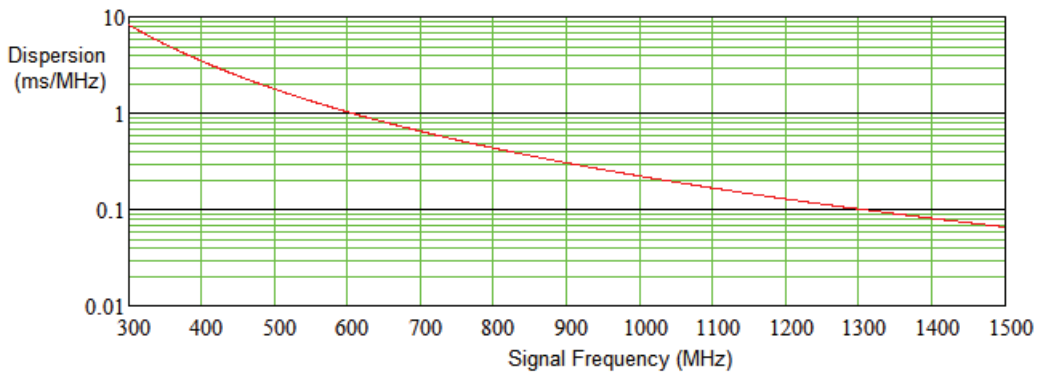

Figure 1. B0329 Dispersion in ms/MHz RF Bandwidth

Figure 1 plots the dispersion for B0329 as a function of radio frequency showing the cubic dependency. In practice, for RF bandwidths below 10 MHz, the local slope can be approximated by its mean value, calculated at the RF band center frequency without any significant reduction in de-dispersion accuracy.
At 610 MHz the slope is close to 1 ms/MHz for DM = 26.7 but at 400 MHz the dispersion slope rises to approximately 3.5 ms/MHz. These figures are applied in the relevant bands in the de-dispersion process.
The effect of dispersion is to reduce the pulse amplitude and broaden the observed (folded) pulse width due to the lower frequencies natural delay. Modeling, using a Gaussian target pulse shape as a function of time, *P(t)*, the pulse amplitude and broadening can be analyzed from the mean pulse response in a period,

$$P(t) = \frac{1}{Nf} \sum_{n=-\frac{Nf}{2}}^{\frac{Nf}{2}} A(n) \exp\left(-4\ln(2) \left[\frac{\left(t - t_0 + \frac{n}{Nf} d \right)}{W} \right]^2 \right) \qquad (2)$$

where,

Nf is the number of RF sub-bands.
n is the sub-band number.
A(n) is the average pulse amplitude in sub-band *n.*
d is the test dispersion in ms in searching across the pulse response.
t_0 is the pulse center time-of-arrival.
W is the pulsar pulse half-height width in ms.

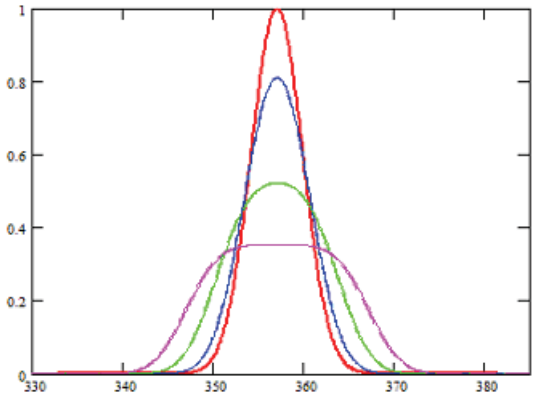

Figure 2. Dispersion Search Effects, *d*/*W* = 0, ±1, ±2, ±3 (red, blue, green, magenta)

Figure 2 illustrates the effect of dispersion on the folded pulse. If the dispersion (t_d x Bandwidth from Equation 2) equals twice the pulse duration, then the folded pulse amplitude (green curve) drops to about one half and the folded pulse width is approximately doubled. In practice, for weaker signals, due to RF scintillation, the underlying noise and a using only few bands, the Figure 2 plots will be distorted, but the general features predicted will be there as shown in Figure 3. Note that noise peaks may change in amplitude and position but do not follow the pattern of a regular pulse train.

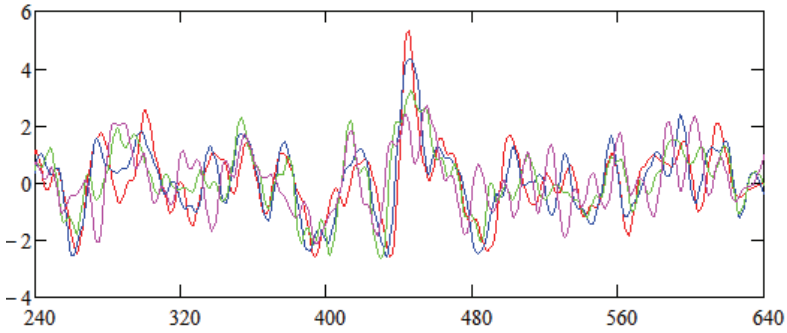

Figure 3. 5.5:1 SNR B0328 Data Dispersion Search Fold, *d*/*W* = 0,±1,±2,±3.

Continuing the 610MHz RF and 10MHz bandwidth example, the propagation dispersion across the band is calculated as approximately 10ms; so for the B0329 pulsar with 6.5ms pulse width, we can expect the non-de-dispersed folded pulse peak to be reduced in amplitude by about one third compared with the correctly de-dispersed result, proving that proper de-dispersion, for 600MHz and below, is a worthwhile exercise.

Practical De-dispersion and Dispersion Search

Data de-dispersion involves separating the received signal bandwidth into a number of sub-bands and delaying the higher sub-bands before video or digital summing to compensate for the interstellar delays. De-dispersion can be carried out at any multi-band stage, including after the channeled data has been separately folded, provided the number of fold bins is adequate for the accuracy required.

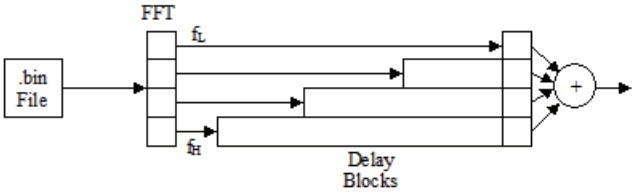

Figure 4. De-dispersion Principle

The principle of de-dispersion is illustrated in Figure 4.

This indicates, using an FFT to divide the raw data band, how the higher frequency components (f_H) are delayed to match the low frequency (f_L) component arrival times and so sum powers to optimize the received SNR. Typically, the data form required for amateur de-dispersion is in multi-band downsampled data samples at rates typically 0.5 to 2 ksps. Using an FFT for band division, the number of frequency channels is usually from 3 to 32 but in this note the investigation is restricted to 3 bands at 1 ksps.

For dispersion measure search, the band delays are varied linearly over a range to accomplish both positive and negative dispersions; the combined data SNR is then calculated to produce a plot similar to the red crossed plot in Figure 5. The blue curve plots the expected folded pulse amplitude using Equation 2 with t_0 = 0, *Nf* = 3, *W* = 6.5 ms and *d* in steps of 1 ms.

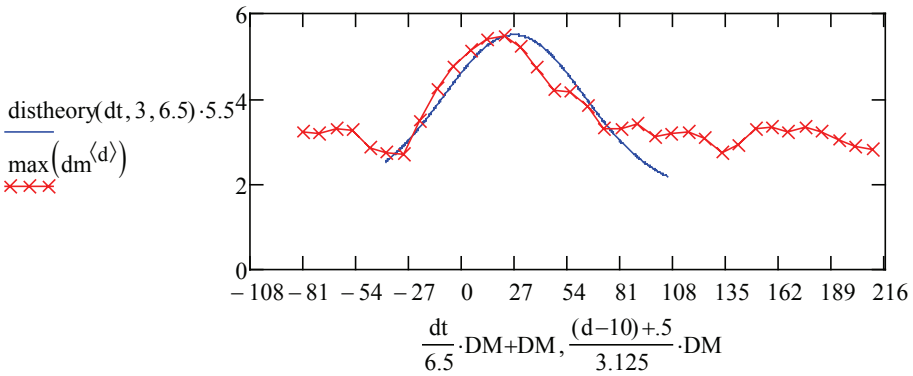

Figure 5. B0329 Dispersion Measure Search. red - Measured Peak Data; blue - Gaussian Pulse Theory

The 10 MHz measurement band was originally divided into 16 bands but since band zero was corrupt, it was ignored and the remaining band of 9.375 MHz was divided into 3 bands approximately 3.125 MHz each (this figure is used in Figure 5 for conversion of ms delay *d* values to *DM*).

In this SNR = 5.5:1 example, the function used to produce the red curve in Figure 5 is listed in Equation 3. *V1*,*V2*, and *V3* are the 3 sub-band folded resultants; each folded into *K* = 714 bins. *q* is the bin number variable and *d* the inter-band delay variable. The delay variable is offset by *d* = 10 ms to allow for negative DM values.

$$dm_{q,d} := V1_{mod(q+K+10-d,K)} + V2_{mod(q,K)} + V3_{mod(q+K-10+d,K)} \qquad (3)$$

(Note: the *mod* function cycles the data delay variable subscript, (q+...) with the period K).

For each value of the delay variable *d*, the combined folded data was scanned and the maximum recorded for the plot. With 714 bins, and approximately 714.5 ms B0329 pulsar period, each bin represents approximately 1 ms so it is relatively easy to convert the delay variable *d* to equivalent DM value. It is noted that the center band V2 is unmodified ensuring that the pulsar pulse peak position is unchanged with the dispersion variable *d*.

Note that the red data plot in Figure 5 peaks close to the expected DM = 26.7 value for B0329 and has a reasonable match to the theoretical shape. Some distortion is expected at this low SNR value due to the influence of the background noise. Outside the peak, the maximum amplitude falls due to the pulse position spread and appears to settle around an equivalent SNR of about 3.5. This is higher than expected for natural noise peaks and is due to using only 3 bands, where for an SNR of 5.5, the average band SNR expected is 5.5/√3 = 3.2:1. The most important verification indicator is the search peak being close to the expected DM value of 26.7.

It seems from Figure 6 that the largest fold peak candidate passes the DM search test. Incidentally, it also passes the pulse width and TEMPO topocentric period matching tests.

From the folded data plot in Figure 6, the pulse candidate appears at bin 445. However, the DM search amplitude discrimination in Figure 5 is not all that great (5.5/3.5 = 1.6:1) and is expected to degrade for lower SNR intercepted observations.

For reference, Figure 6 plots the example's raw folded SNR results for the 3-band data and (below) their de-dispersed sum.

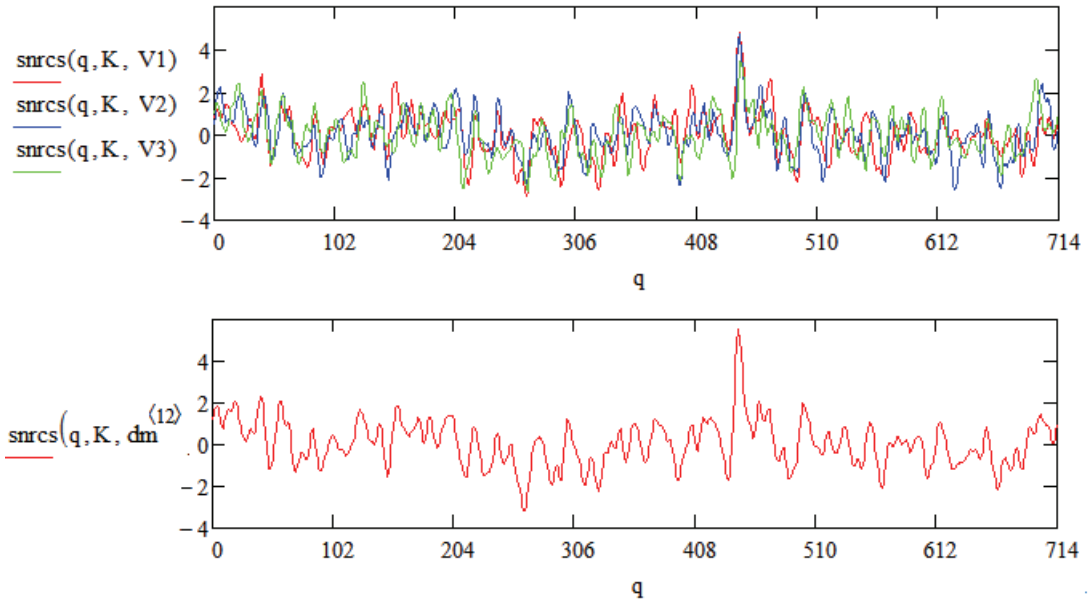

Figure 6. B0329 Folded Data. Upper: Band folded results; Lower De-dispersed Full Result (SNR = 5.5:1)

Viewing the upper plot in Figure 6, there is a useful pulsar signal response at bin 445 in all bands but some obvious correlation exists between the base noises of the three plots, together with some low frequency mean drift. Both these latter issues, probably attributable to the power supply, can be mitigated and so improve the summed resulting SNR. This has not been done for this exercise but for information, with optimal peak/spur thresholding, the non de-dispersed sum SNR increased from 5.1:1 to 5.5:1.

Sub-band Choice

For the tests described in this note, the measurement band data was divided into just three bands, for convenience of this description and analysis. Five-band division and seven-band division was also evaluated (see Appendix 1) together with increasing the time delay resolution from 1 ms to 0.5 ms.

Some improvement was noted in these cases, mainly in the search scan peak moving closer to the expected DM figure.

Improving Search Discrimination

A simple check that it is indeed the candidate pulse that is responsible for the dispersion search peak around DM = 26.7 is to blank the pulse response around the candidate bin 445 and repeat the search routine.

The theoretical curve in Figure 7 and the peak tracking curve remain as Figure 5, but it is seen that blanking the candidate at bin position 445 (purple curve - fold bins 440 to 450 zeroed) completely removes the peak of the red curve response showing that the pulse around bin position 445 is indeed responsible. Subtracting the red and purple plots now produces the black curve which is identified as the DM contribution of the nulled candidate peak. This gives a much clearer indication that pulse at bin 445 peaking around DM = 26.7 confirms the dispersion measure expected for pulsar B0329.

Blanking any other peak potential candidate selected in Figure 6 produces a negligible or zero black curve difference (in this case, the pulse candidate's delayed components always dominate).

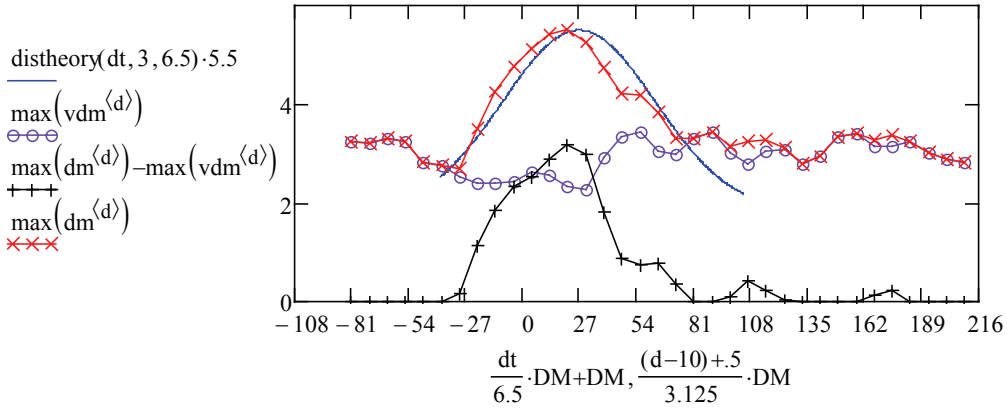

Figure 7. B0329 Dispersion Measure Search.
blue - Gaussian Pulse Theory; red - Original Peak Data, purple - Pulse removed, black - Difference

Data Evaluation

In a previous article it was noted that the cumulative SNR plot added insight into the scintillation nature of the pulsar and the growth of SNR in the folding integration process [5]. For the present data this is plotted in Figure 8 (red curve).

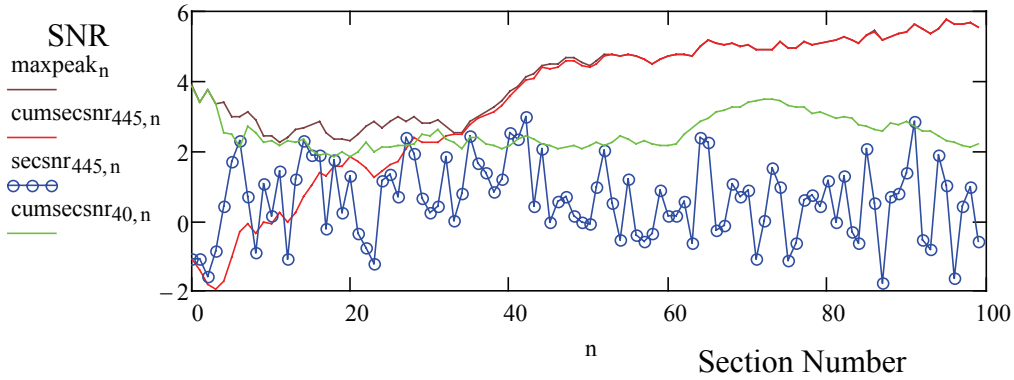

Figure 8. Cumulative Peak SNR (brown) , Pulsar target (red) and Section SNR (blue)

In Figure 8, the data is divided into 100 sections, each section is folded and the SNR calculated to produce the blue circle points. It is noticed that whilst appearing random due to scintillation and base noise, there is a positive mean offset. This offset mean should track the accumulated SNR of the whole data record divided by 10 (= √100). The brown curve represents the accumulated section peak SNR as a function of the number of sections integrated. Finally the red curve showing a rising amplitude trend accumulates the section SNR of bin number 445, the bin occupied by the candidate target. This shows that the candidate takes over the integrated peak by about section number 35. There are several regions of sharp candidate

rises which can be attributed to strong scintillation. There are some negative sloping regions where the target signal is weak or subsumed in background noise.
The green curve plots the cumulative SNR of the next strongest fold candidate at bin 40 (see Figure 6) and the gentle flattish rolling trend appears typical of random noise spikes. This tendency of noise peaks persisting at a modest level is also evident in the cumulative waterfall presentations (see results in Section 2 below).

Testing the New DM Search Discriminator
The presentation in Figure 8 (blue circles, section SNR), identifies both good and bad sections contributing to the integration of the candidate pulsar. It therefore seems feasible to artificially modify some of the worst sections for indicating the candidate presence and either zero them to remove their influence and enhance the final wanted SNR or alternatively, increase them to further degrade the section and final SNR (see SNR discussion in Appendix 2). By this means, we can examine the ruggedness of the proposed DM discriminator. The pulsar candidate's eighteen lowest (negative) SNR valued fold patterns of the one hundred section SNRs were identified for modification.
These were sections: 0,1,2,3,8,12,22,23,57,63,66,71,75,76,87,92,93,96.
The test involves dividing the identified bad sections by the factor 100 to reduce their influence and improve the target SNR or multiplying the section fold amplitudes by the factor 1.8 to increase their influence and degrade the final SNR.

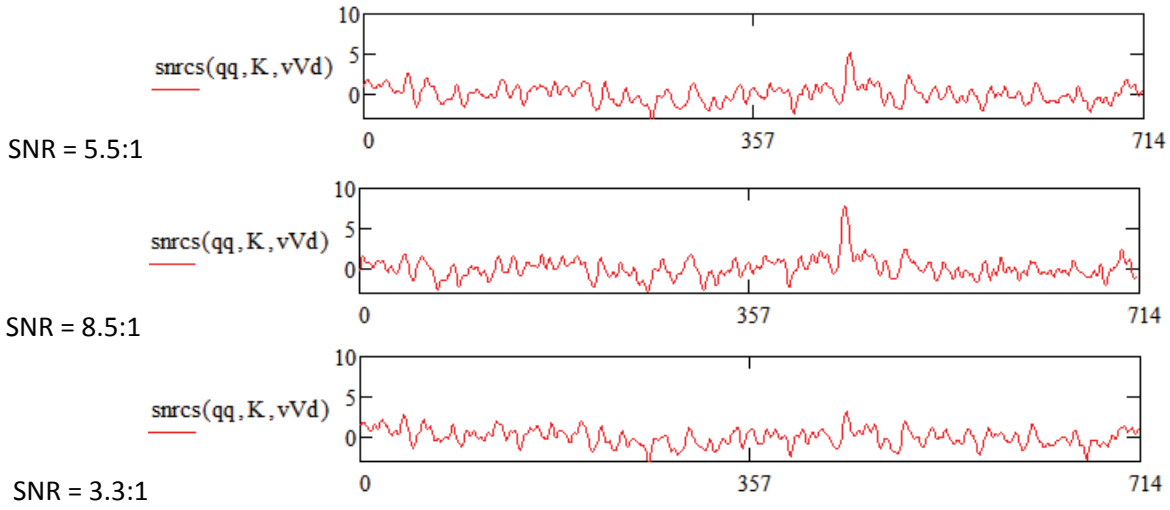

Figure 9. Selected Sections Reduced by the Factor 100 (8.5:1) and Increased by the factor 1.8 (3.3:1)

The result of these noise-section modification actions seen in Figure 9 are firstly, to increase the target candidate SNR from 5.5:1 (top plot) to 8.5:1 (center plot), and finally to reduce the target SNR to 3.3:1 (lower plot). It is noted in both cases that the folded base noise is largely the same and the pulse shape appears unaffected.

Other candidate noise peaks can be investigated in this way. For each candidate, large negative SNR corresponding sections are removed/reduced and searches repeated. Removal of these sections increases the relative amplitude of the candidate to the natural fold response, allowing it to be the main subject of the parameter search. It may be necessary to blank the main peak to ensure this condition.

Figure 10 shows the DM search consequences for the two extreme SNR DM plots.
For the enhanced SNR case, the DM search peak more closely matches the Gaussian pulse theoretical solution; the peak moving closer to DM = 26.7. As a validation measure, confidence in this case can be very high. For the degraded SNR case the basic (red crosses) DM search is inconclusive, a peak around DM = 26.7 is still visible but it is not the largest peak scanned (occurring at DM = -81). What is evident with this low SNR, is that when blanking around the known target bin, an amplitude reduction over the region is now obvious and that with the suggested new discrimination method (black crosses), a clear peak still appears

around the expected DM value albeit at a low amplitude figure. Blanking any other fold peak candidate produces no response around DM = 26.7.

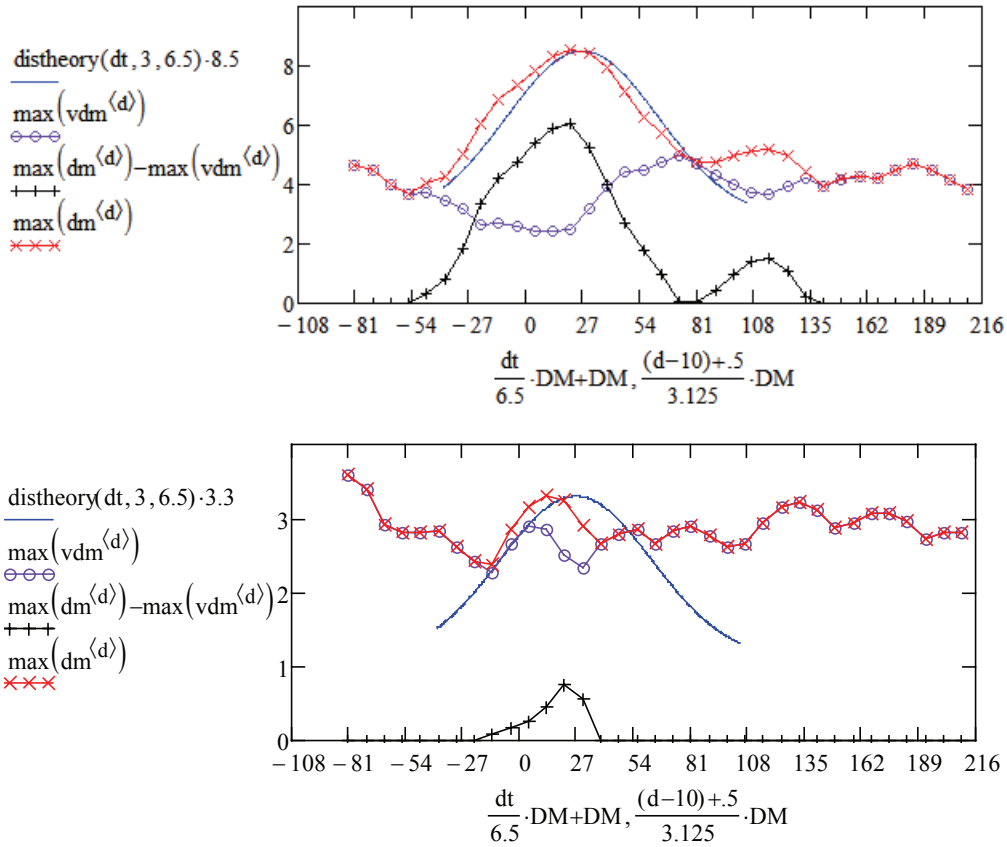

Figure 10. DM Search Plots for the Cases of Enhanced (upper plot) and Degraded (lower plot) Data SNRs

Section 2 contains the full PRESTO validation simulation charts for the three cases.

***Section 2*. Results - PRESTO Simulation Plots**

PRESTO Sub-plot Validation - Introduction

The PRESTO *prepfold* program produces a graphical display of sub-plots from which the known pulsar characteristics can be compared for validation.

In summary, they are,

1a. Profile - Confirms correct topocentric period, correct pulse width, duty cycle and shape.
1b. Time Waterfall – Evidence of continuous, scintillating pulse train.
1c. Cumulative section power - Increasing trend confirms continuous scintillating pulse train.
2. Frequency Waterfall – Evidence of wide band source. (also scintillation with many bands)
3a. Period Search - Peak at zero confirms period matching accuracy.
3b. P-dot Search - peak at zero confirms high stability pulse train.
3c. 2D Period/P-dot plot - Central negative slope ridge confirms pulsar period and stability.
5. DM Plot - Peak around expected DM figure confirms extra-terrestrial source.

A clear indication in all sub-plots is necessary to ensure that all the expected pulsar characteristics are visibly confirmed without ambiguity before target validation is affirmed. Typically for pulsars with duty cycles around 100:1 the intercept integrated SNR for PRESTO needs to be above 10:1. This figure is reduced for lower duty cycle pulsars. Prior to running the PRESTO *prepfold* software, part of PRESTO involves running software such as *rfifind* to locate and minimize the effects of sporadic RFI and RF spurs/birdies. The PRESTO RFI mitigation processes are not clear but plots are usually optimized by repeated *prepfold* runs adjusting set software variables to optimize the final SNR.

The plots have been duplicated in this Section using MathCad representations of the PRESTO features but using peak folded SNR amplitude sensing rather than the Chi-square statistic to monitor pulsar power.

Results 1. As Recorded Data - Integrated Apparent SNR = 5.5:1

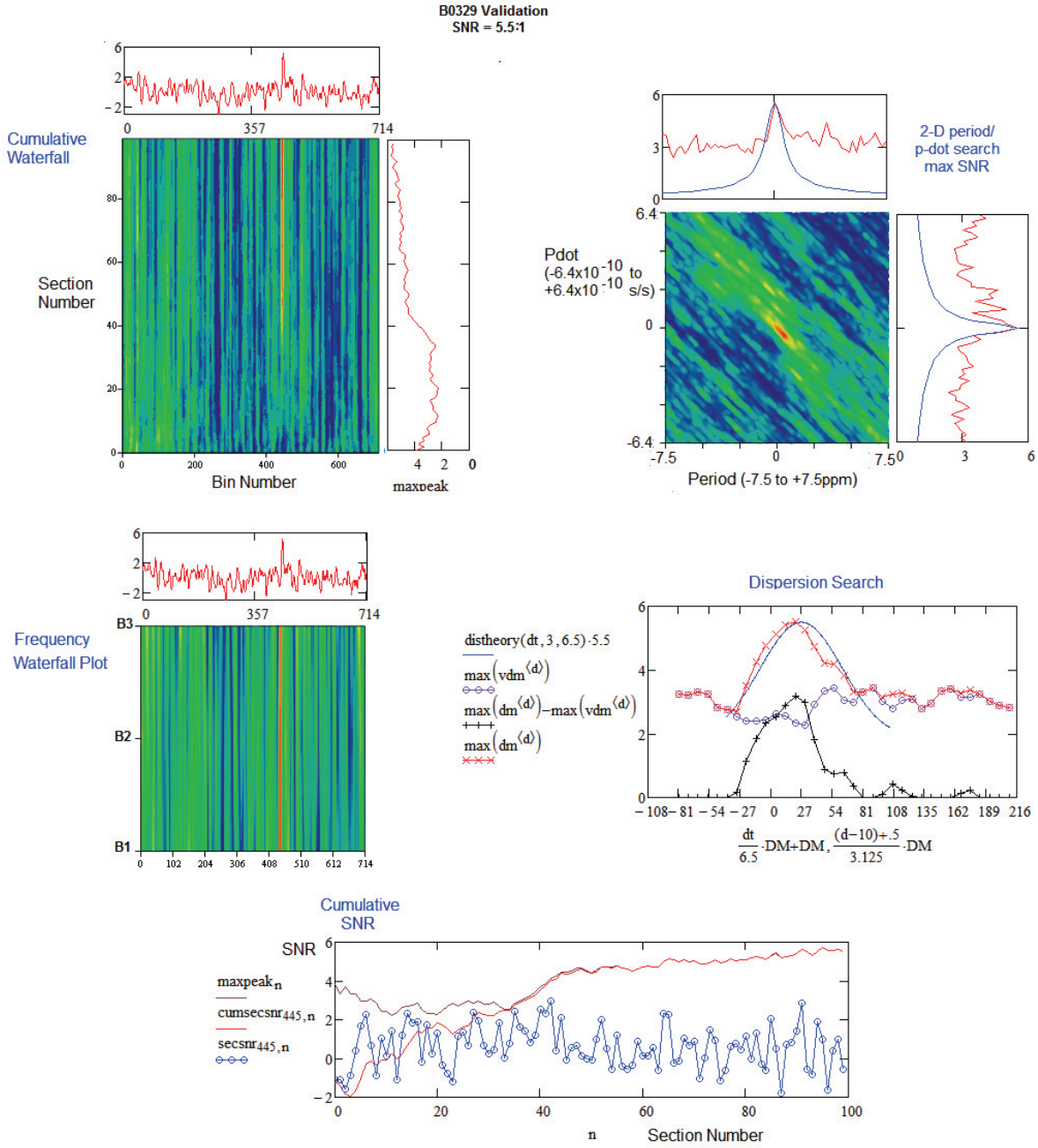

Notes for Data 5.5:1 SNR:

1. Cumulative Waterfall - The red line indicates that from about section 35. the integrated bin position 445 is becoming dominant resulting in the profile pattern above. The green noise streaks noted appear typical of persistent natural folded noise peaks that once established maintain a fairly flat profile. Around section 70 a typical noise peak grows in bin 40 and highlighted in Figure 8 (green plot).
2. Frequency Waterfall - Strong result in all three bands. Some noise correlation is evident, possibly due to power supply ripple.
3. 2D Period/P-dot - Peaks at the center zero for both period and p-dot. 2D display coordinates chosen so that the expected high-point ridge lies at 45 degrees for ease of visualization. Strong response observed.
4. Dispersion search - Good peak visible. New discriminator shows strong response around DM = 26.7.
5. Cumulative SNR - Steady rising integration.
6. Overall - Strong positive pulsar indications in all sub-plots.

Results 2. Bad Data Sections Nulled - Integrated Apparent SNR = 8.5:1

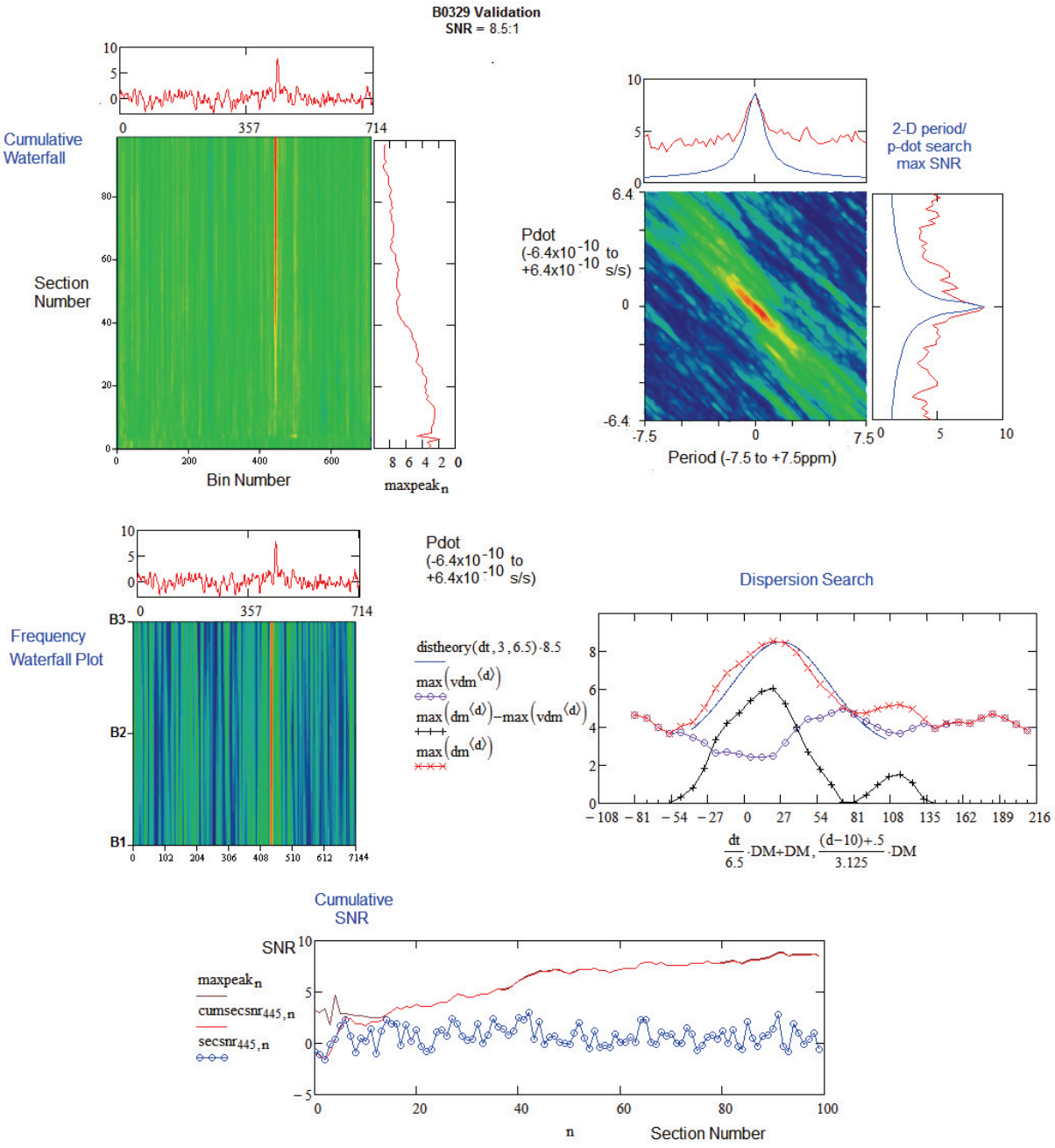

Notes for Data 8.5:1 SNR:

1. Cumulative Waterfall - Superior integrated SNR at bin position 445. Profile peak enhanced. The green noise streaks suppressed although some lines are persistent. Note that the base noise pattern although suppressed by the increased SNR is still moderately correlated over the sections.
2. Frequency Waterfall - Very strong result in all three bands. Noise/PSU ripple correlation still evident.
3. 2D Period/P-dot - Peaks at zero for both period and p-dot. 2D display coordinates set so that the more significant high-point ridge lies at 45 degrees. Very strong response.
4. Dispersion search - Strong peak more closely aligned to the theoretical curve. New discriminator shows stronger response around DM = 26.7.
5. Cumulative SNR - Steady rising integration. Largest effect seems to be due to the blanking of the first few sections - confirmed by re-analysis of the data file with the front end of the data file removed.
6. Overall - Strong positive pulsar indications in all sub-plots.

Results 3. Bad Data Sections Further Degraded by Factor 1.8 - Integrated Apparent SNR = 3.3:1

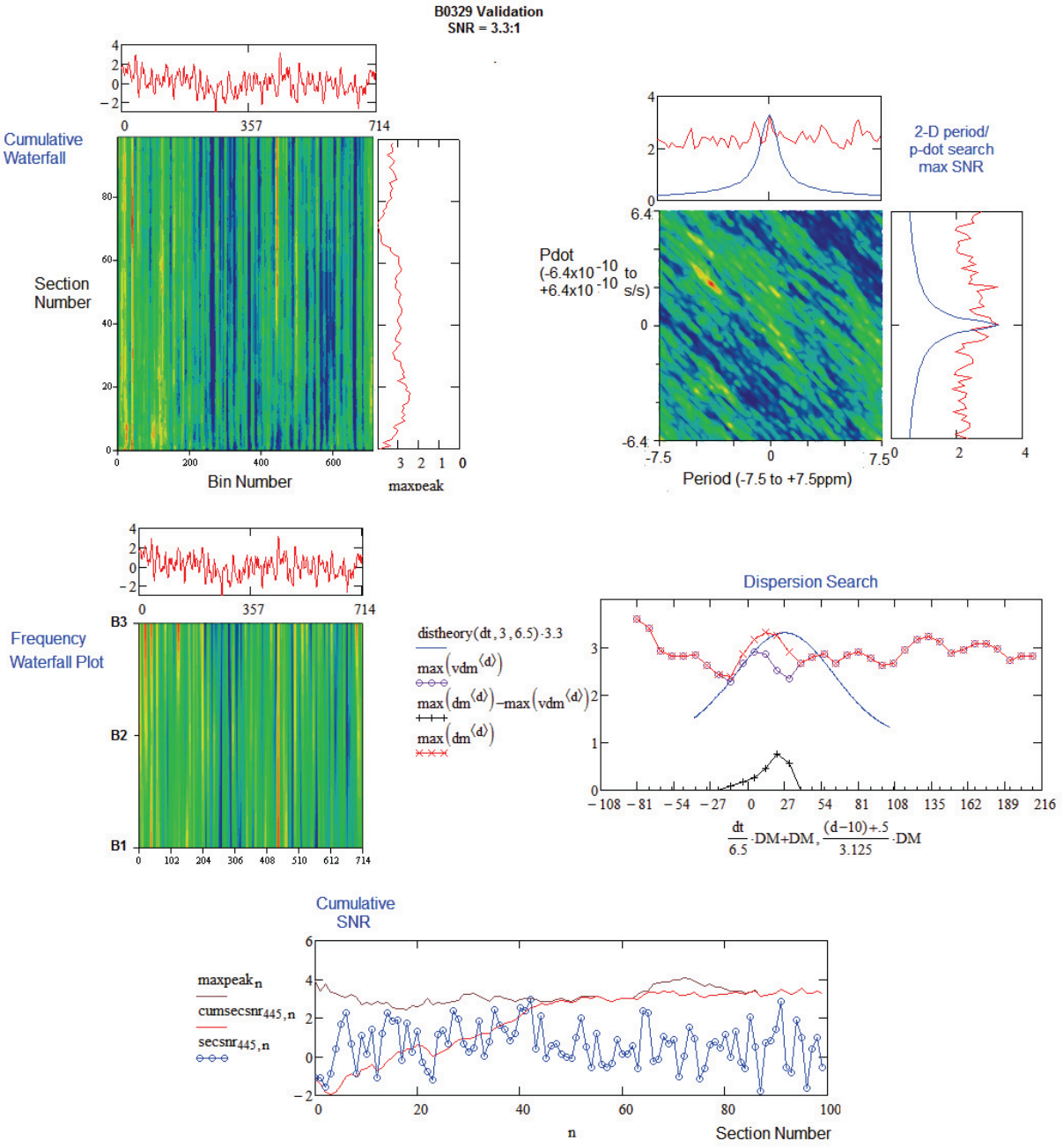

Notes for Data 3.3:1 SNR:

1. Cumulative Waterfall - The red line rising later around section 40 and showing evidence of some scintillation. Integration of the strongest component is still at bin position 445. Some noise streaks are competing now and the peak at bin 40 is more evident.
2. Frequency Waterfall - Good correlation of bin 445 in all bands but reduced in band 3 where other noise peaks are competing.
3. 2D Period/P-dot - Peaks at zero for both period and p-dot plots, although the background discrimination is poor. 2D display just showing evidence of a ridge (yellow) at the center (0,0) with the expected -45^{o} slope.
4. Dispersion search - An unambiguous peak is still present although the peak a much lower than the expected value due to the influence of the base noise. The new discriminator shows a modest response but peaking closer to DM = 26.7. The new discriminator rejects the stronger noise peak of bin 40.
5. Cumulative SNR - Steady rising integration for bin 445 but indicating that the integrating noise peak of bin 40, for a short range, actually exceeds bin 445 final SNR.
6. Overall - Positive pulsar indications in all sub-plots.

Results 4. Gaussian Noise Only - Integrated Apparent SNR = 3.25:1

For completeness, as this is a real issue, the validation regime was tested with just Gaussian noise of the same amplitude as the data recorded. In most trials the various sub-plots showed little evidence of a pulse-like signal. To encourage some ambiguity, after many random trials, one was selected and the search period adjusted to ensure a peak occurred in center of the 2-D period/p-dot plot and at the same time, a peak occurred at the DM expected for B0329. The resulting plot and discussion is listed below.

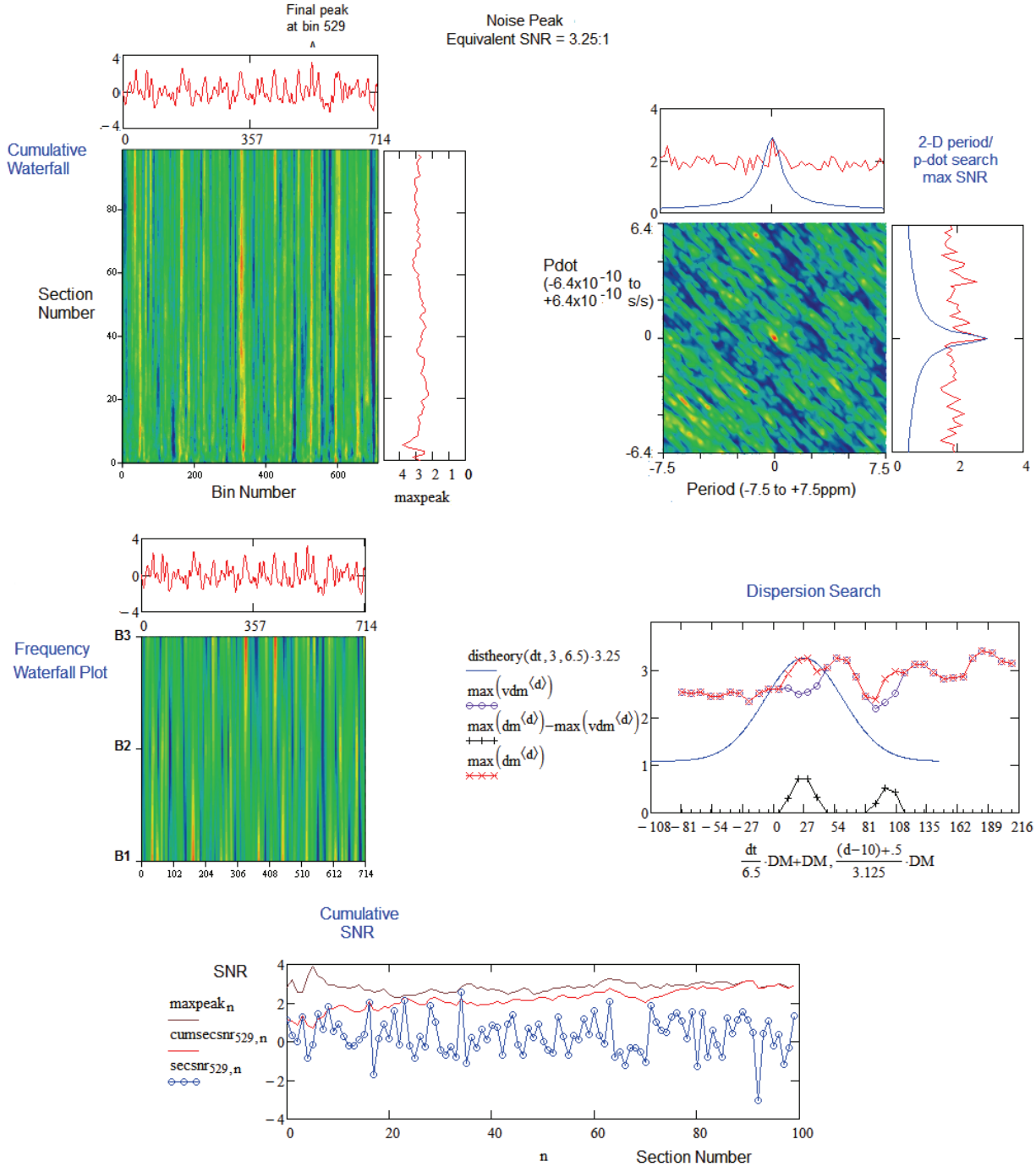

Notes for Noise 3.25:1 SNR:

1. Cumulative Waterfall - Shows the growth of bin 529 peak and rising earlier than the response of Result 3. The early generation and persistence of noise peaks seems to be an intrinsic property of the folding algorithm. Initially the accumulated noise peaks appear random but by about a fifth of the range they seem established.
2. Frequency Waterfall - A faint line (SNR ~ 2:1) visible in all three bands but is overshadowed by higher peaks at other bins. Providing a noise peak is coincident in all bands, that bin will integrate linearly on summing.
3. 2D Period/P-dot - Noise data selected to ensure peaks at the center. Other peaks apparent. Little evidence of an extended -45^{o} slope ridge.

4. Dispersion search - Noise data selected to generate a peak the DM of B0329. The new discriminator shows and confirms the match too.
5. Cumulative SNR - Major difference between Results 3 and 4 is the response of the selected peak at bin 529. A fairly flat even response is typical of a noise component. Even with weak scintillating true pulsars, an upward trend is usually seen as in the Results 3 section.
6. Overall - Ambiguous pulsar-like indications in most sub-plots - further investigation is necessary.

Section3. Concluding Comments

Conclusions

It has been shown that by the simple procedure of zero-blanking the extent of the pulsar candidate and repeating the full dispersion search routine on folded sub-band data, then their difference, identifies the candidates unique contribution to the dispersion measure plot with superior discrimination confidence.

Further pulsar validation confidence can be gained if the data is divided into sections and folded cumulatively. Characteristics typical of a pulsar include a rising integrated SNR trend; also, scintillation can be inferred by noting the presence of discrete positive and negative slopes.

It has also been shown that for chosen candidate peaks, bad folded sections are identified by large negative section-SNRs and if these are nulled, an increased candidate peak results which can be better tested using the standard parameter search processes. On the other hand, these bad sections can be amplified so reducing the perceived SNR to further extend full search evaluation.

PRESTO *prepfold* type graphics for the three real data SNR cases are presented in Section 2; all illustrate positive pulsar-matching characteristics in all the sub-plots.

As a caution, the three band data was replaced with uncorrelated Gaussian noise sets specially selected to pass the period, p-dot and DM search tests and the results are presented in Results 4. This exercise proved that at very low SNRs, ambiguity is always a possibility but can be mitigated with care. Increasing the number of bands will reduce the probability of noise peaks correlating constructively, as in this case and there are other subtle differences that can be exploited. Probably the most surprising observation was the persistence and near-constant level of noise peaks in the cumulative waterfall/SNR plots. RFI ambiguity was not observed in the analyzed data set, so not examined.

Postscript

This journey through the jungle of low SNR pulsar validation has proved very rewarding and confirmed admiration for the academics that developed the PRESTO software many years ago. For amateurs, once you have proved your receiver sensitivity, the scintillating property of pulsar signal propagation means that observation success can be very variable. By correctly directing the antenna, at the right time and duration, you know it will always be there and with a forensic set of software tools, you can often find it. Some of the ideas and methods offered have proven difficult concepts for some, but all are based on the standard folding algorithm and honest use of data. Folding tens or hundreds of gigasamples of received data to a few hundred points and relying on statistics for validation, ignores much useful information on the way.

Detailed understanding of the properties of both pulsars and noise is the means to finding this flashing needle in the cosmic haystack.

References

[1] PRESTO Home, https://www.cv.nrao.edu/~sransom/presto/

[2] SM Ransom. Searching for Pulsars with PRESTO https://www.cv.nrao.edu/~sransom/PRESTO_search_tutorial.pdf

[3] PW. East, Getting the Best out of the PRESTO Pulsar Search & Analysis Tools., Journal of the Society of Amateur Radio Astronomers. January-February 2021.

[4] PW. East, Getting the Best out of PRESTO - Part 2 The PRESTO Period/P-Dot Search Graphic., Journal of the Society of Amateur Radio Astronomers. March-April 2021.

[5] PW East, Getting the Best out of PRESTO - Part 3: Waterfalls and Conclusions., Journal of the Society of Amateur Radio Astronomers. July-August 2021.

Appendix 1. DM Search Sensitivity to Number of Sub-Bands

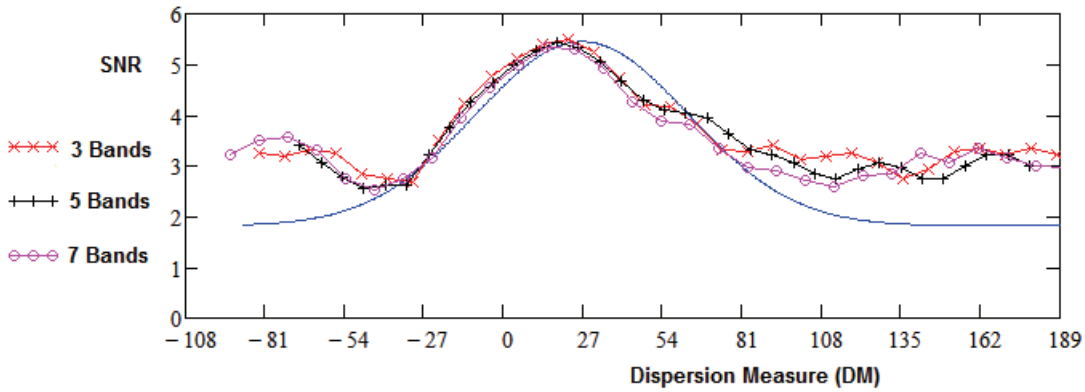

Figure A1. DM Search Plots with 3, 5 and 7 Sub-bands

Figure A1 compares the DM search sensitivity to changing the number of sub-bands and shows for the 10 MHz RF receiver band, that there is very little variation between 3, 5 and the 7 sub-band split. This confirms that in this case, reducing the number of sub-bands to three to minimize the computation load is a valid simplification.

Appendix 2. True SNR?

The apparent SNR of the candidate pulsar in the data explored here was modified to check DM search tolerance by identifying bad sections of the data and either reducing or increasing their influence on the candidate pulsar integration process. Whilst this accomplished the aim by decreasing and increasing the base noise relative to the pulsar candidate power, so modifying the apparent SNR, it doesn't shed any light on the data true SNR. The SNR measured for any data set is the sum of the integrated candidate signal and the local bin noise (which may be positive or negative) divided by the standard deviation of the integrated noise. The latter is usually calculated from the folded noise outside the effective pulse width. Normal folded noise peaks can typically be within the range ±2 standard deviations, so the measured SNR can be anywhere in the range of the true SNR ±2.

For low SNR measurements, natural selection favors finding pulsars sitting on natural folded noise peaks and this is sometimes evident from noisy search measurements of period, p-dot and dispersion.

In this case, all the parameter search match discriminations improved when bad sections were removed. Noise and RFI peaks can also be enhanced with this technique for peak isolation and easing candidate search investigations.

PW East. January 2022

Peter East, *pe@y1pwe.co.uk* is retired engineer after a career of radar and electronic warfare system design. He has had a lifelong interest in radio astronomy; lately active in amateur detection and recognition of pulsars at low SNR. Novel parameter recognition algorithms that better flag pulsar features in noise have been published in the Journal to encourage members to take up the challenge. Intercepting the strongest pulsar in either hemisphere is no longer the privilege of big-aperture amateurs.

His active website is at *http://www.y1pwe.co.uk* and he is happy to answer questions.